Study Session on Quantum Computation of Quantum Chemistry

Yuan-Chung Cheng
鄭原忠

Department of Chemistry
National Taiwan University

NTU Chemistry Building, Room 215
October 4, 2018

Paper #2

PHYSICAL REVIEW X **6,** 031007 (2016)

Scalable Quantum Simulation of Molecular Energies

P. J. J. O'Malley,[1,*] R. Babbush,[2,†] I. D. Kivlichan,[3] J. Romero,[3] J. R. McClean,[4] R. Barends,[5] J. Kelly,[5] P. Roushan,[5] A. Tranter,[6,7] N. Ding,[2] B. Campbell,[1] Y. Chen,[5] Z. Chen,[1] B. Chiaro,[1] A. Dunsworth,[1] A. G. Fowler,[5] E. Jeffrey,[5] E. Lucero,[5] A. Megrant,[5] J. Y. Mutus,[5] M. Neeley,[5] C. Neill,[1] C. Quintana,[1] D. Sank,[5] A. Vainsencher,[1] J. Wenner,[1] T. C. White,[5] P. V. Coveney,[7] P. J. Love,[6] H. Neven,[2] A. Aspuru-Guzik,[3] and J. M. Martinis[5,1,‡]

- Algorithms and experiments on the simulation of H_2 dissociation curve (John Martinis, Josephson Junction Quantum Computing, UCSB & Google)
- Read-outs based on variational quantum eigensolver & phase estimation algorithm are both tested
- Jordan-Wigner transformation/Bravyi-Kitaev transformation/Trotterization/VQE/iterative PEA/CI space reduction/unitary coupled cluster

Different Types of Qubits

Physical support	Name	Information support	$\|0\rangle$	$\|1\rangle$
Photon	Polarization encoding	Polarization of light	Horizontal	Vertical
	Number of photons	Fock state	Vacuum	Single photon state
	Time-bin encoding	Time of arrival	Early	Late
Coherent state of light	Squeezed light	Quadrature	Amplitude-squeezed state	Phase-squeezed state
Electrons	Electronic spin	Spin	Up	Down
	Electron number	Charge	No electron	One electron
Nucleus	Nuclear spin addressed through NMR	Spin	Up	Down
Optical lattices	Atomic spin	Spin	Up	Down
Josephson junction	Superconducting charge qubit	Charge	Uncharged superconducting island (Q=0)	Charged superconducting island (Q=2e, one extra Cooper pair)
	Superconducting flux qubit	Current	Clockwise current	Counterclockwise current
	Superconducting phase qubit	Energy	Ground state	First excited state
Singly charged quantum dot pair	Electron localization	Charge	Electron on left dot	Electron on right dot
Quantum dot	Dot spin	Spin	Down	Up
Gapped topological system	Non-abelian anyons	Braiding of Excitations	Depends on specific topological system	Depends on specific topological system

And many more!!

https://en.wikipedia.org/wiki/Qubit#Physical_implementations

Superconducting qubits – a timeline

1911 Heike Kamerlingh Onnes
Superconductivity in He

1933 Walter Meissner
"Meissner effect"

1957 Bardeen, Cooper, Schrieffer
Theory of Superconductivity

1962 Supercurrent through a non-superconducting gap

1997 Schnirman et al. – theoretical proposal for JJ qubits

1998 Devoret group (Saclay)
first Cooper Pair Box qubit

1999 Nakamura, Tsai (NEC)
Rabi oscillations in CPB

2000 Lukens, Han (SUNY SB)
Flux qubit

2002 Martinis (NIST)
phase qubit

2006 Martinis (UCSB)
two-qubit gate (87% fidelity)

https://pdfs.semanticscholar.org/presentation/5203/cf0422ce4e8ceee08ee7fcd9e5bbcd615f4e.pdf

Flux quantization

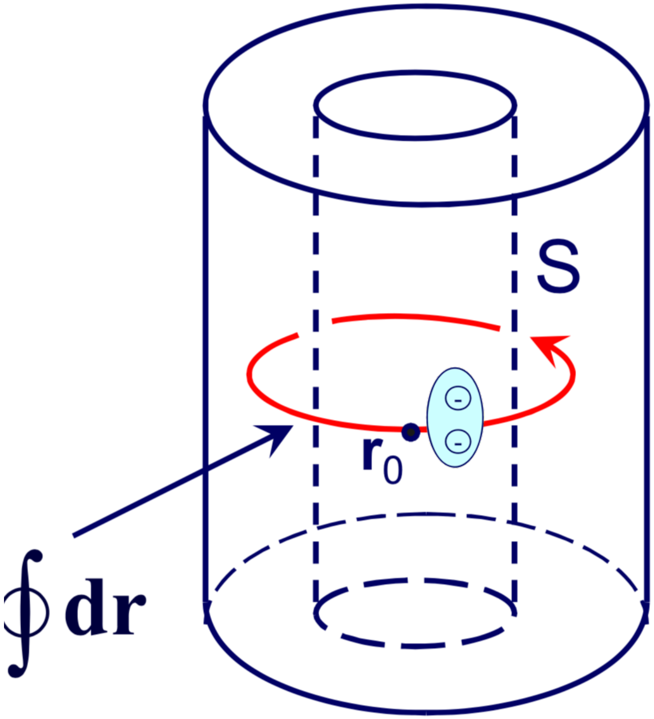

$$\psi'(\mathbf{r}) = \psi^{(0)}(\mathbf{r}) e^{(i2e/\hbar)\int_{\mathbf{r}_0}^{\mathbf{r}} \mathbf{A}(\mathbf{r}')\, d\mathbf{r}'}$$

$$\frac{2e\Phi}{\hbar} = 2n\pi \rightarrow \boxed{\Phi = \frac{n\pi\hbar}{e}},$$

$$n = 0, 1, 2, \ldots$$

Josephson Junction

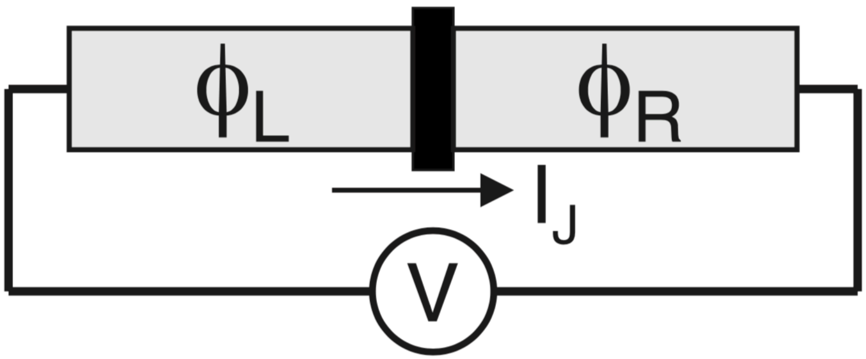

$$I_J = I_0 \sin \delta$$

Figure 1. Schematic diagram of a Josephson junction connected to a bias voltage V. The Josephson current is given by $I_J = I_0 \sin \delta$, where $\delta = \phi_L - \phi_R$ is the difference in the superconducting phase across the junction.

Phase Qubit

Equations that define the Josephson junction:

Classical:

$$I_J = I_0 \sin\delta$$
$$V = \frac{\Phi_0}{2\pi}\frac{d\delta}{dt},$$

Quantum:

$$H = \frac{1}{2C}\widehat{Q}^2 - \frac{I_0\Phi_0}{2\pi}\cos\widehat{\delta} - \frac{I\Phi_0}{2\pi}\widehat{\delta}$$

$$[\widehat{\delta}, \widehat{Q}] = 2ei$$

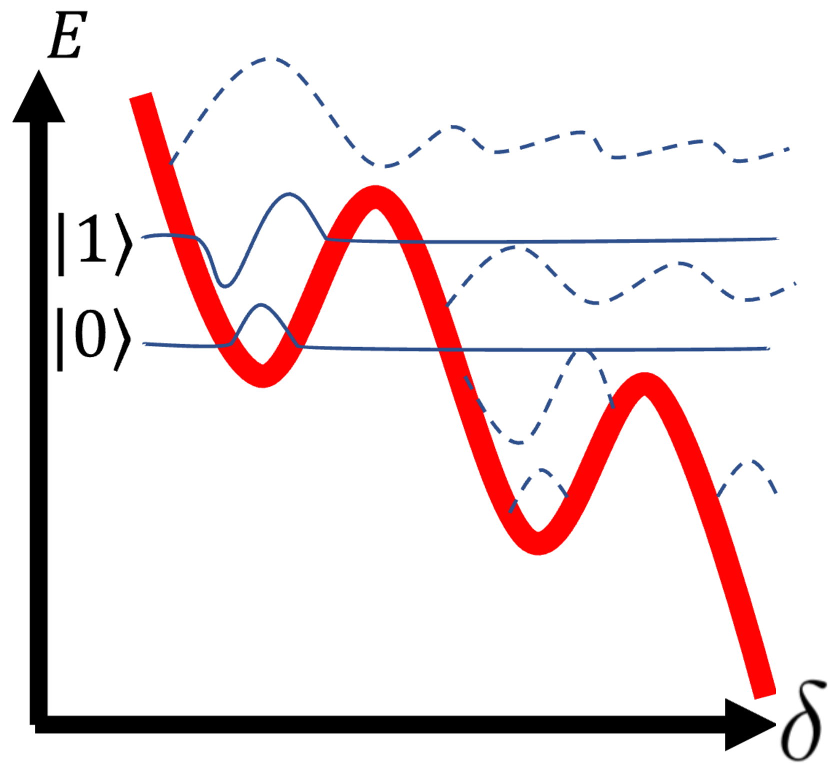

Physical Implementation

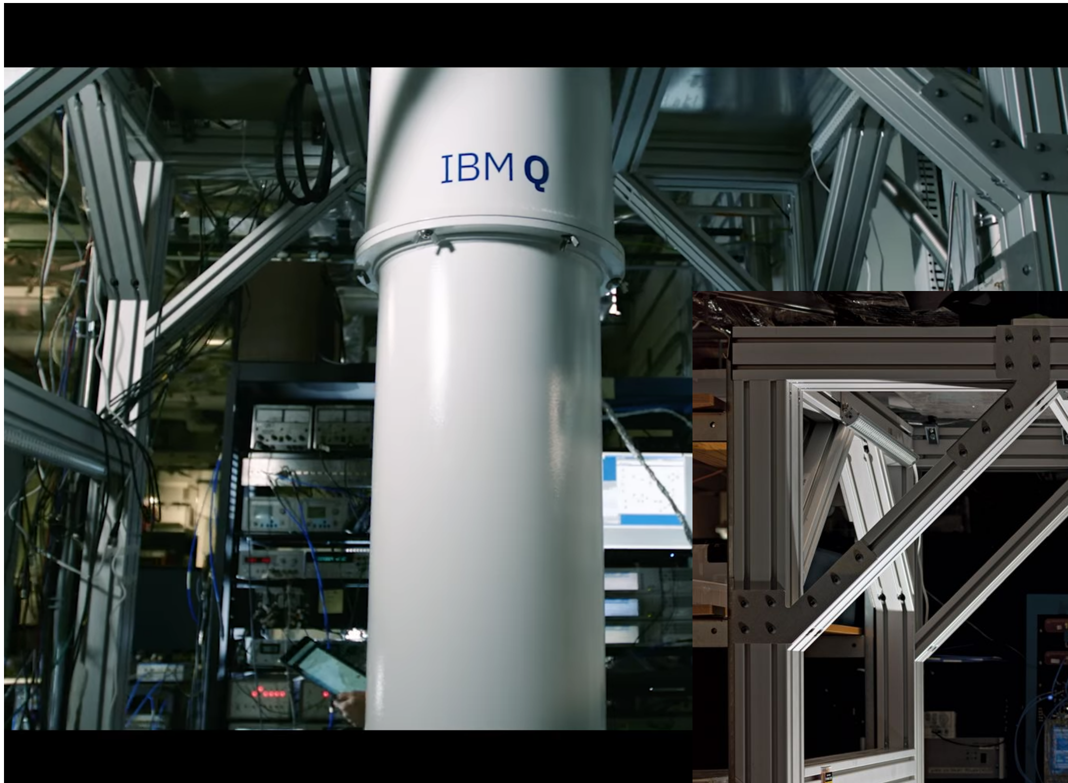

Physical Implementation

LETTER

doi:10.1038/nature17658

Digitized adiabatic quantum computing with a superconducting circuit

R. Barends[1], A. Shabani[2], L. Lamata[3], J. Kelly[1], A. Mezzacapo[3]†, U. Las Heras[3], R. Babbush[2], A. G. Fowler[1], B. Campbell[4], Yu Chen[1], Z. Chen[4], B. Chiaro[4], A. Dunsworth[4], E. Jeffrey[1], E. Lucero[1], A. Megrant[4], J. Y. Mutus[1], M. Neeley[1], C. Neill[4], P. J. J. O'Malley[4], C. Quintana[4], P. Roushan[1], D. Sank[1], A. Vainsencher[4], J. Wenner[4], T. C. White[4], E. Solano[3,5], H. Neven[2] & John M. Martinis[1,4]

Nature 534, 222 (2016).

Physical Implementation

QUANTUM INFORMATION

A blueprint for demonstrating quantum supremacy with superconducting qubits

C. Neill,[1*†] P. Roushan,[2*] K. Kechedzhi,[3,4] S. Boixo,[2] S. V. Isakov,[2] V. Smelyanskiy,[2] A. Megrant,[2] B. Chiaro,[1] A. Dunsworth,[1] K. Arya,[2] R. Barends,[2] B. Burkett,[2] Y. Chen,[2] Z. Chen,[1] A. Fowler,[2] B. Foxen,[1] M. Giustina,[2] R. Graff,[2] E. Jeffrey,[2] T. Huang,[2] J. Kelly,[2] P. Klimov,[2] E. Lucero,[2] J. Mutus,[2] M. Neeley,[2] C. Quintana,[1] D. Sank,[2] A. Vainsencher,[2] J. Wenner,[1] T. C. White,[2] H. Neven,[2] J. M. Martinis[1,2†]

A key step toward demonstrating a quantum system that can address difficult problems in physics and chemistry will be performing a computation beyond the capabilities of any classical computer, thus achieving so-called quantum supremacy. In this study, we used nine superconducting qubits to demonstrate a promising path toward quantum supremacy. By individually tuning the qubit parameters, we were able to generate thousands of distinct Hamiltonian evolutions and probe the output probabilities. The measured probabilities obey a universal distribution, consistent with uniformly sampling the full Hilbert space. As the number of qubits increases, the system continues to explore the exponentially growing number of states. Extending these results to a system of 50 qubits has the potential to address scientific questions that are beyond the capabilities of any classical computer.

Neill et al., Science 360, 195–199 (2018)

Physical Implementation

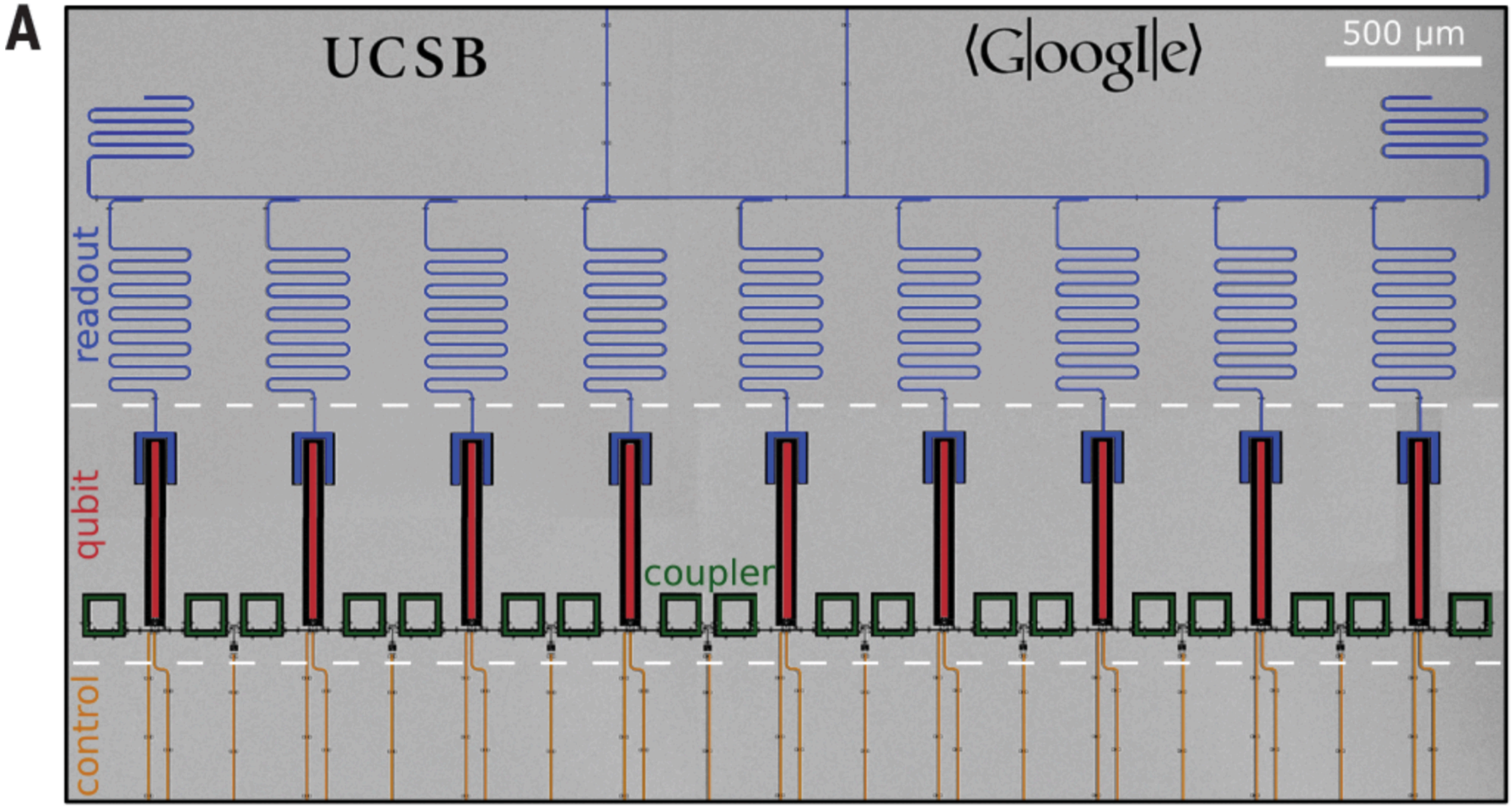

Neill et al., Science 360, 195–199 (2018)

Physical Implementation

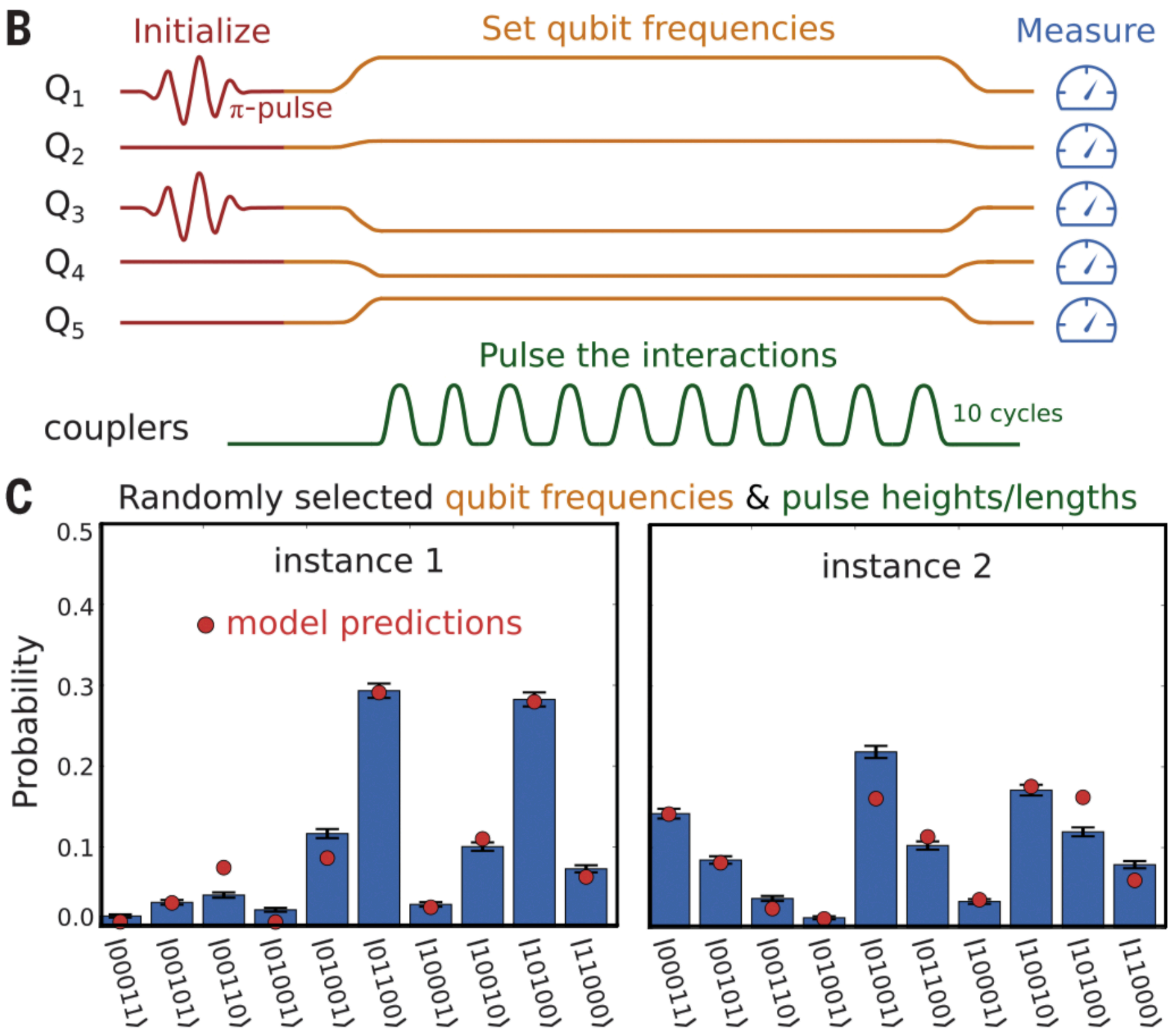

(C) We repeat this pulse sequence for randomly selected control parameters. Each instance corresponds to a different set of qubit frequencies, coupling pulse heights and lengths. Here we plot the measured probabilities for two instances after 10 coupler pulses (cycles). Error bars (±3 SD) represent the statistical uncertainty from 50,000 samples. Predictions from a control model are overlaid as red circles.

Neill et al., Science 360, 195–199 (2018)

Physical Implementation

Fig. 3. Fidelity: learning a better control model.
(**A**) Average fidelity decay versus number of cycles for five- to nine-qubit experiments (circles). The fidelity is computed from Eq. 3. The error per cycle, presented in the inset, is the slope of the dashed line that best fits the data. (**B**) Using the fidelity as a cost function, we learn optimal parameters for our control model. We take half of the experimental data to train our model. The other half of the data is used to verify this new model; the optimizer does not have access to these data. The corresponding improvement in fidelity of the verification set provides evidence that we are indeed learning a better control model.

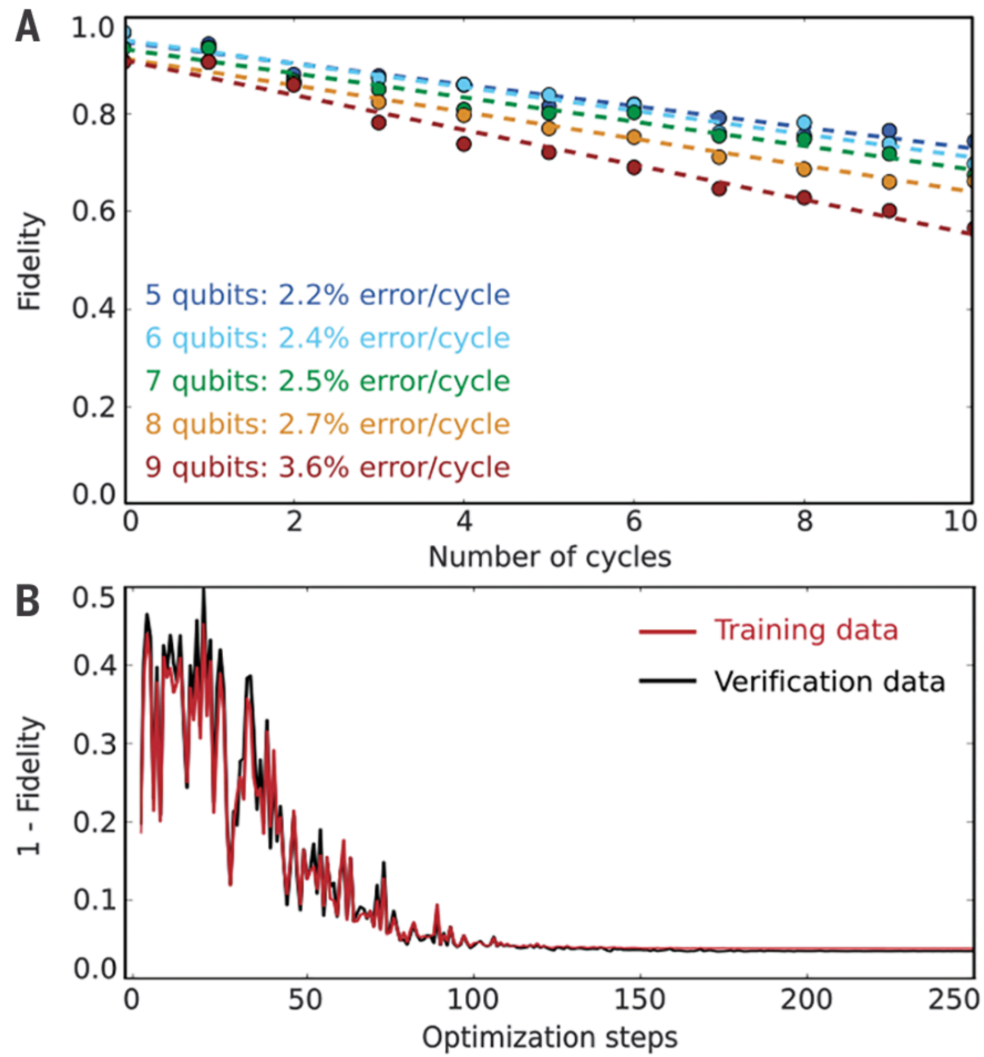

Neill et al., Science 360, 195–199 (2018)

Physical Implementation

npj Quantum Information

www.nature.com/npjqi

ARTICLE OPEN

3D integrated superconducting qubits

D. Rosenberg[1], D. Kim[1], R. Das[1], D. Yost[1], S. Gustavsson[2], D. Hover[1], P. Krantz[2], A. Melville[1], L. Racz[1], G. O. Samach[1], S. J. Weber[1], F. Yan[2], J. L. Yoder[1], A. J. Kerman[1] and W. D. Oliver[1,2,3]

As the field of quantum computing advances from the few-qubit stage to larger-scale processors, qubit addressability and https://doi.org/10.1038/s41534-017-0044-0 extensibility will necessitate the use of 3D integration and packaging. While 3D integration is well-developed for commercial electronics, relatively little work has been performed to determine its compatibility with high-coherence solid-state qubits. Of particular concern, qubit coherence times can be suppressed by the requisite processing steps and close proximity of another chip. In this work, we use a flip-chip process to bond a chip with superconducting flux qubits to another chip containing structures for qubit readout and control. We demonstrate that high qubit coherence (T_1, $T_{2,echo} > 20$ μs) is maintained in a flip-chip geometry in the presence of galvanic, capacitive, and inductive coupling between the chips.

npj Quantum Information (2017)3:42 ; doi:10.1038/s41534-017-0044-0

Physical Implementation

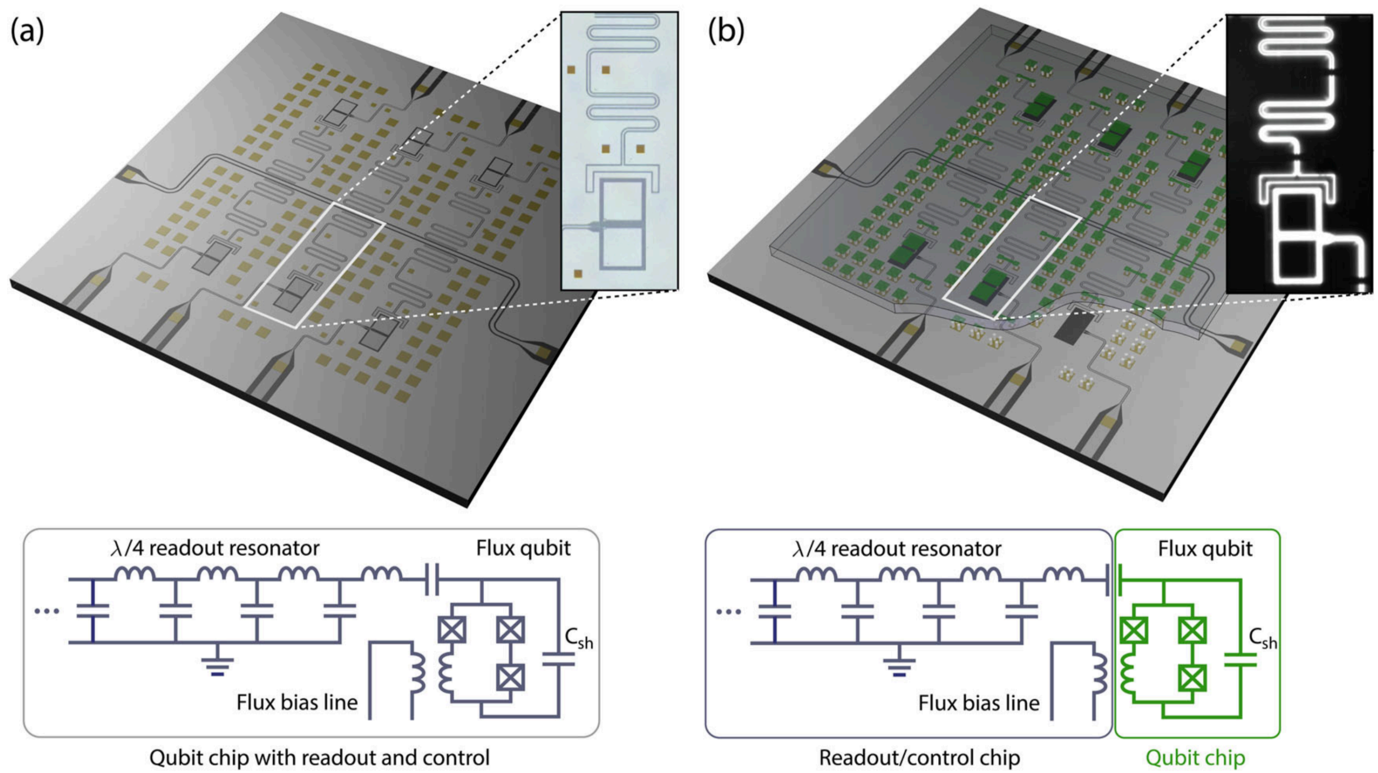

Fig. 2 Standard (**a**) and flipped qubit chip (**b**) configurations. **a** Schematic of standard qubit chip with six capacitively shunted flux qubits. Each qubit, which comprises a loop with three Josephson junctions shunted by a large capacitor, is capacitively coupled to a quarter-wave resonator for dispersive readout and control, and inductively coupled to a flux bias line. In this configuration, all readout and control elements are on the qubit chip. The array of small squares are the under bump metallization layer. An optical micrograph of one of the qubits and its corresponding readout resonator is shown to the right. **b** Schematic of a flip-chip qubit chip. In this configuration, the qubits are on one chip, whereas the readout and control elements are on another chip that is bonded to the qubit chip. For visibility, the metal on the qubit chip is shown in green in the schematic and on the circuit diagram. An infrared through-chip image of one of the qubits and readout resonators is shown to the right. The features which appear to be breaks in the resonator and bias lines are strips of metal on the qubit chip to connect different sections of ground plane on the readout and control chip

Physical Implementation

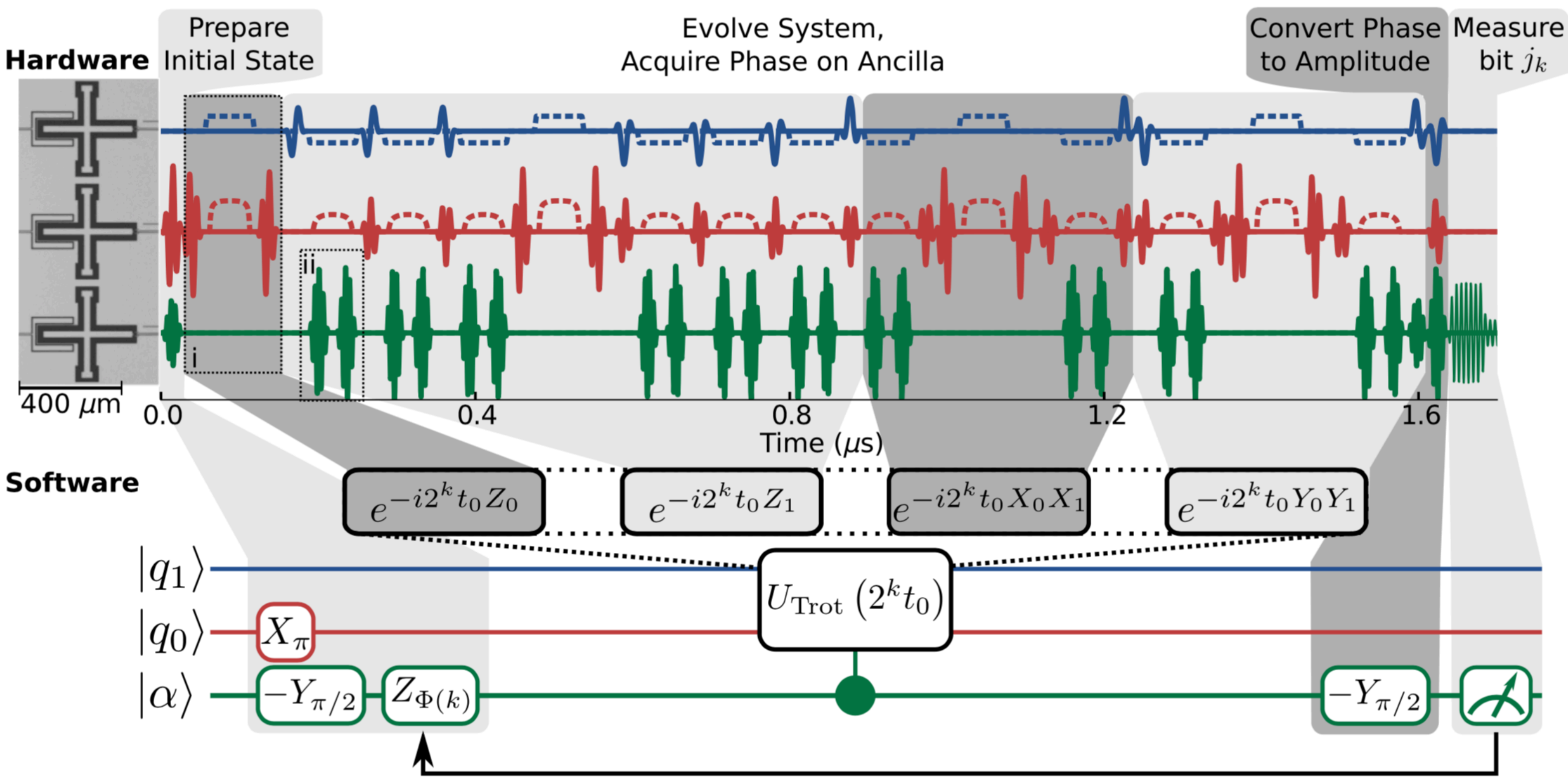

FIG. 4. Hardware and software schematic of the Trotterized phase estimation algorithm. (Hardware) micrograph shows three Xmon transmon qubits and microwave pulse sequences, including (i) the variable amplitude CZ_ϕ (not used in Fig. 1) and (ii) dynamical decoupling pulses not shown in logical circuit. (Software) state preparation includes putting the ancilla in a superposition state and compensating for previously measured bits of the phase using the gate Z_{Φ_k} (see text). The bulk of the circuit is the evolution of the system under a Trotterized Hamiltonian controlled by the ancilla. Bit j_k is determined by a majority vote of the ancilla state over 1000 repetitions.